FORMATION OF THE LARGE-SCALE MAGNETIC FIELD AND PREDICTION OF ACTIVITY CYCLES

© 2025 A. G. Tlatov*, I. A. Berezin, K. A. Tlatova

Kislovodsk Mountain Astronomical Station, GAO RAS, Kislovodsk, Russia.

**e-mail: tlatov@mail.ru*

Received February 24, 2025

Revised April 22, 2025

Accepted June 17, 2025

Abstract. To predict solar activity, the method of precursors is used. One such precursor is the polar field precursors. On the other hand, there are indications that the amplitude of the subsequent solar cycle is related to low-latitude activity. Within the framework of the surface magnetic flux transport model, we reproduce supersynoptic maps in latitude-time coordinates. We show that for selected transport parameters, including the diffusion coefficient D = 500 km^2/s, the meridional circulation rate u_θ~10 m/s , and the tilt-angle of magnetic bipoles τ~10°, there exists a latitude θ1 at which the magnetic field from regions of leading polarity penetrates into the opposite hemisphere and a dipole magnetic field of the Sun is formed. When θ > θ1, the magnetic field does not penetrate into the opposite hemisphere and the large-scale magnetic field at the poles remains negligible with time. The value of θ_1 is in the range 10-20º. Active regions with latitude θ < θ1 are most important for the next activity cycle. We proposed prognostic indices to predict the amplitude of activity cycles based on sunspot data in the current activity cycle with a correlation coefficient r > 0.8.

Keywords: *solar, large-scale magnetic field, flux transport model, prediction*

DOI: 10.31857/S00167940250717e8

1. INTRODUCTION

Various methods are currently used to make long-term forecasts of solar activity. One method that has produced forecasts within the correct range of values over the last few solar cycles is the polar precursor method [Jiang et al., 2023]. The polar precursor method is based on the correlation between the amplitude of the sunspot maximum with a measure of the amplitude of the magnetic field near the poles of the Sun at the minimum of the previous cycle. It is based on the causal relationship between the toroidal flux and the poloidal flux, which serves as a seed for the generation of toroidal fields by twisting the field lines in the differentially rotating convective zone. It is now widely accepted that the polar precursor method is the most reliable way of predicting the upcoming solar cycle. Near-pole magnetic field observations have been regularly observed at

Mount Wilson Observatory since 1974, Wilcox Solar Observatory (WSO) since 1976, and Kitt Peak since 1976 (since 2003 SOLIS), the STOP magnetograph at Kislovodsk since 2014. The most widely used set of direct measurements of the magnetic field in the polar regions of the Sun is the WSO magnetograph [Petrovay, 2020]. There are indirect tracer data of polar magnetism covering much longer time scales. For example, polar plumes [Tlatov, 2009], which are now considered good photospheric proxy data for polar magnetic field/flux reconstructions.

On the other hand, there are indications that the amplitude of solar cycles is related to low-latitude activity. Thus in [Javariah, 2007, 2023] it was found that the sum of the areas of sunspot groups in the latitude range 0° -10° of the southern hemisphere during a short interval (7-9 months) after the maximum of a solar cycle correlates well with the amplitude of the next solar cycle.

Thus, there is some contradiction between the approaches for predicting solar activity. At first glance, it is difficult to make a connection between polar and low-latitude precursors used to predict the next activity cycles. In this paper, based on modeling the near-field magnetic flux transport, we will try to resolve these contradictions.

2. MODELING OF MAGNETIC FLUX TRANSPORT AT THE SURFACE

The surface flux transport model (hereafter SFT) is based on an idea originally formulated by Leighton [Leighton, 1964]: the radial magnetic flux at the solar surface behaves as a passive scalar field. This means that the flux is carried by horizontal plasma fluxes, but with no feedback on these fluxes. The SFT model has been successful in reproducing the magnetic flux structure at the real solar surface (photosphere). In general, the success of the SFT model has led to important applications both as an internal boundary condition for extrapolating the magnetic field in the solar atmosphere and as an external boundary constraint for models of the Sun's internal dynamo.

We have implemented the SFT model using a difference scheme similar to [Caplan et al., 2025]. Using the SFT model, we studied the role of magnetic flux transport of the fields of the leading AR regions across the equator for the formation of a dipole-type field [Tlatov et al., 2024].

Figure 1 shows a comparison of the latitude-time diagram of the distribution of the large-scale magnetic field from STOP magnetograph observations and SFT modeling. Supersynoptic maps are presented in this figure. To create them, the magnetic field is not averaged over longitude, but the longitude interval near the central meridian corresponding to the moment in time is cut out on the magnetograms (Fig. 1a). For modeling, the main flux parameters to be chosen are the meridional flux profile $u_\theta(\theta)$ and the diffusion coefficient D.

The character of the magnetic flux in the SFT model is largely determined by a given term $S(\theta,\varphi,t)$, which represents the appearance of new macroscopic active regions on the surface [Yeates et al., 2023]. For this simulation, we used sources from active regions with magnetic field $|B| > 30$ Gs. The diffusion coefficient was assumed to be $D = 500\ km^2/s$. With the chosen parameters, the latitude-time SFT model (Fig. 1b) fits the observed time-latitude plot (Fig. 1a) well at all latitudes. The comparison indicates that our and the model and the approach itself to the question of the formation of the Sun's large-scale magnetic field are sufficiently reliable. One of the conclusions that can be drawn is that the large-scale magnetic field is a product of the evolution of the magnetic fields of active regions and has no other sources.

Since the classical SFT equation is linear with respect to Br [Tlatov et al., 2024], the solution is a superposition of solutions for each individual active region, so it is reasonable to consider separately the evolution of one of these regions.

Traditionally, SFT models consider each active region as a bipolar magnetic region (BMR), with circular flux patches centered at the local poles (θ-, φ-) and (θ+, φ+) [Jiang et al., 2023]. This representation is consistent with Joy's law in the sense that the leading polarity is closer to the equator. Figure 2 shows the surface magnetic field variation plots for the trial bipoles at latitude θ = 10° and latitude θ = 30°. The tilt-angle was chosen to be $\tau\sim10°$, diffusion coefficient η = 500 km^2/s, meridional velocity with amplitude $u_\theta\sim10$ m/s and differential rotation according to [Caplan et al., 2025]. We see a significant difference in the behavior of the surface magnetic field. For a bipole at relatively high latitude θ = 30° the field at the north pole tends to zero with time. For a low-latitude bipole θ = 10° the Sun's magnetic field becomes dipole-like with time. By fitting, we found that for the chosen model parameters, bipoles at latitudes less than $\theta1\sim20°$ can form a polar magnetic field. Bipoles with latitude $\theta > \theta1$ do not contribute to polar fields.

As we know from dynamo theories, the dipole large-scale field is the source of a new cycle of activity [Yeates et al., 2023]. Thus, we can assume that only low-latitude active regions generate a dipole-type polar magnetic field and hence influence the next activity cycle.

3. PREDICTING SOLAR ACTIVITY

We can construct predictive indices based on the hypothesis of different contributions of active regions depending on their latitude. We used sunspot group data from the RGO/UASF data for the period N:13-25 activity cycles (http://solarcyclescience.com/activeregions.html).

Figure 3 shows such indices. In Fig. 3a, the median latitude of AO $<\theta>$ is used. The formula we used to calculate the index can be represented as $(\theta cr-<\theta>)\sum S$, where the summation over the areas of spot groups is performed for all spots in the cycle. The latitude $\theta1$ found by fitting was θcr= 20.0^o, with a correlation coefficient with the amplitude of the next cycle of r= 0.864. Figure 3b shows another index that takes into account ARs with latitude less than $\theta_{cr} < 13°$. In this index, the spot area of the current cycle is included with a degree $\sum S^4$. The correlation coefficient of the index with the amplitude of the subsequent cycle was r= 0.89.

Both prognostic indices include a critical latitude θ_{cr}. The more ARs with latitude less than this value $\theta < \theta_{cr}$, the larger the expected amplitude of the next activity cycle. By amplitude we have here considered the total area of the AO. The existence of latitude θ_{cr} is consistent with our assumption from the SFT simulations. AOs at latitudes $\theta>\theta_{cr}$ have little effect on the formation of the large-scale dipole-type field, because due to the transfer to high latitudes, the magnetic fields of the positive and negative parts of the bipoles remain in this hemisphere. Since the total magnetic flux from pop-up ARs is zero, the large-scale field eventually becomes insignificant (see Fig. 2a and Fig. 2b). In the case of ARs at low latitudes, due to diffusion, part of the magnetic field of decaying ARs can penetrate through the solar equator (Fig. 2a and Fig. 2b). Since the centers of the parts of ARs of the leading polarity are closer to the equator, magnetic fields of the leading polarity penetrate to the opposite hemisphere. As a consequence, a large-scale magnetic field with unipolar regions at high latitudes of opposite polarity in different hemispheres is formed. It is believed that such a large-scale field is associated with the next activity cycle. The above calculations and the estimate of the critical latitude can be used to refine the diffusion coefficient of the meridional circulation.

4. CONCLUSIONS

We used the surface transport model and properties of active regions, such as Joy's law about the closer location of magnetic fields of leading regions to the equator than of tail regions. We conclude that for active regions there is some threshold latitude θ_1, at which a large-scale dipole-type magnetic field is formed. Active regions at higher latitudes $\theta>\theta_1$do not participate in the formation of the polar magnetic field because their total magnetic flux in the hemisphere where they appeared tends to zero at the poles. On the contrary, for ARs with latitude $\theta<\theta_1$the magnetic flux from the leading regions due to diffusion can cross the solar equator and form a dipole magnetic field. Such a dipole magnetic field participates in the formation of the next activity cycle. Based on this hypothesis, we proposed prognostic indices based on the consideration of low-latitude active regions.

FUNDING

This work was partially supported by the project of the Ministry of Education and Science of the Russian Federation No. 075-03-2025-420/4.

CONFLICT OF INTERESTS

The authors declare that they have no conflict of interest.

REFERENCES

1. *Caplan, R.M., Stulajter M.M., Linker, J.A., Upton L., Jha B.K., Charles A., Arge N., Henney C.J.* Open-source Flux Transport (OFT). I. HipFT–High-performance Flux Transport // The Astrophysical Journal Supplement Series, V. 278, N 1, id.24, 22 pp. 2025. https://doi.org/10.3847/1538-4365/adc080

2. *Javaraiah J.* North–south asymmetry in solar activity: predicting the amplitude of the next solar cycle // MNRAS.V. 377, L34–L38, 2007. https://doi.org/10.1111/j.1745-3933.2007.00298.x
3. *Javaraiah J.* Prediction for the amplitude and second maximum of Solar Cycle 25 and a comparison of the predictions based on strength of polar magnetic field and low-latitude sunspot area // MNRAS. 2023. V. 520, 5586–5599. https://doi.org/10.1093/mnras/stad479
4. *Leighton, R.B.* Transport of Magnetic Fields on the Sun // Astrophys. J., V. 140, pp. 1547–1562. 1964. https://doi.org/10.1086/148058
5. *Petrovay K.* Solar cycle prediction // Living Reviews in Solar Physics, V. 17. No. 2. 2020. https://doi.org/10.1007/s41116-020-0022-z (0123456789-vol.V)
6. *Tlatov A.G., Berezin I.A., Tlatova K.A.* Formation of Near-Surface Magnetic Fields of the Sun // Geomagnetism and Aeronomy, 2024, V. 64, No. 7, pp. 1176-1181. https://doi.org/10.1134/S0016793224700269
7. *Tlatov A.G.* The minimum activity epoch as a precursor of the solar activity // Sol. Phys., V. 260, 465–477. 2009. https://doi.org/10.1007/s11207-009-9451-5
8. *Jiang J., Zhang Z., Petrovay K.* Comparison of physics-based prediction models of solar cycle 25 // Journal of Atmospheric and Solar-Terrestrial Physics. V. 243, article id.106018. 2023
https://doi.org/10.1016/j.jastp.2023.106018
9. *Yeates A.R., Cheung M.,·Jiang J., Petrovay K., Wang Yi-Ming*. Surface Flux Transport on the Sun // Space Science Reviews, v. 219, article id. 31, 2023, https://doi.org/10.1007/s11214-023-00978-8

FIGURE CAPTIONS

Fig. 1. a) Supersynoptic map from STOP magnetograph observations. b) Surface magnetic field modeling

Fig. 2. a) Diagram in latitude-time coordinates for a bipole at latitude $\theta = 10^{o}$ at $\eta = 500$ km^2/s. (b) Magnetic field intensity in the circumpolar regions of the northern and southern hemispheres for (a). (c) Same as (a) but for a bipole at latitude $\theta= 30^{o}$. (d) Same as (b) but for bipole (c).

Fig. 3. Prediction of the amplitude of the next activity cycle in Sum$(S)_n$ as a function of the AO index at low latitudes. a) Index from median latitude $<\theta>$ and threshold latitude 20.5°. b) Index of spots with latitude less than 13 °.

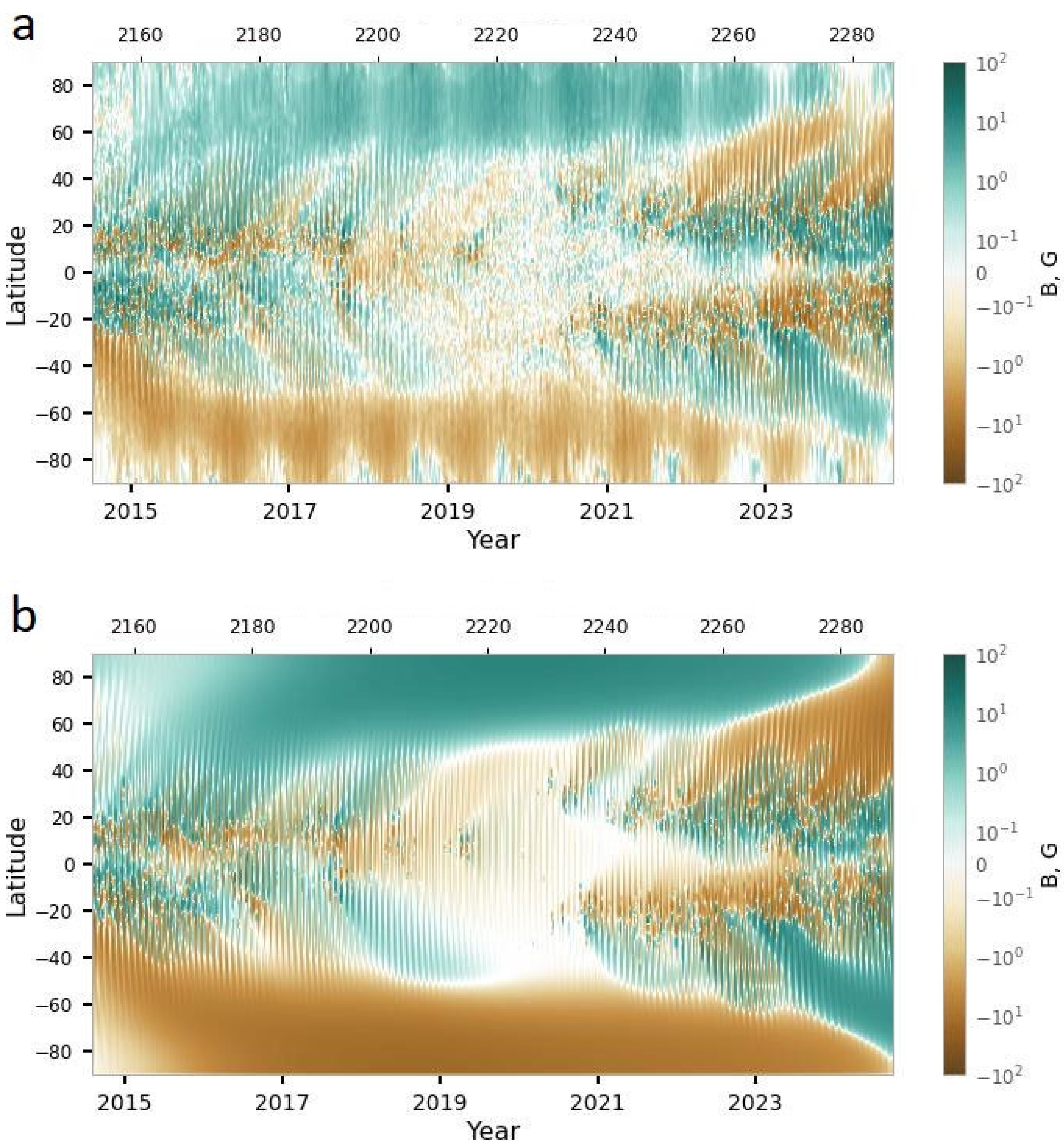

a
2160
2180
2200
2220
2240
2260
2280
80
60
40
20
0
−20
−40
−60
−80
Latitude
2015
2017
2019
2021
2023
Year
10^2
10^1
10^0
10^{-1}
0
-10^{-1}
-10^0
-10^1
-10^2
B, G
b
2160
2180
2200
2220
2240
2260
2280
80
60
40
20
0
−20
−40
−60
−80
Latitude
2015
2017
2019
2021
2023
Year
10^2
10^1
10^0
10^{-1}
0
-10^{-1}
-10^0
-10^1
-10^2
B, G

Fig. 1.

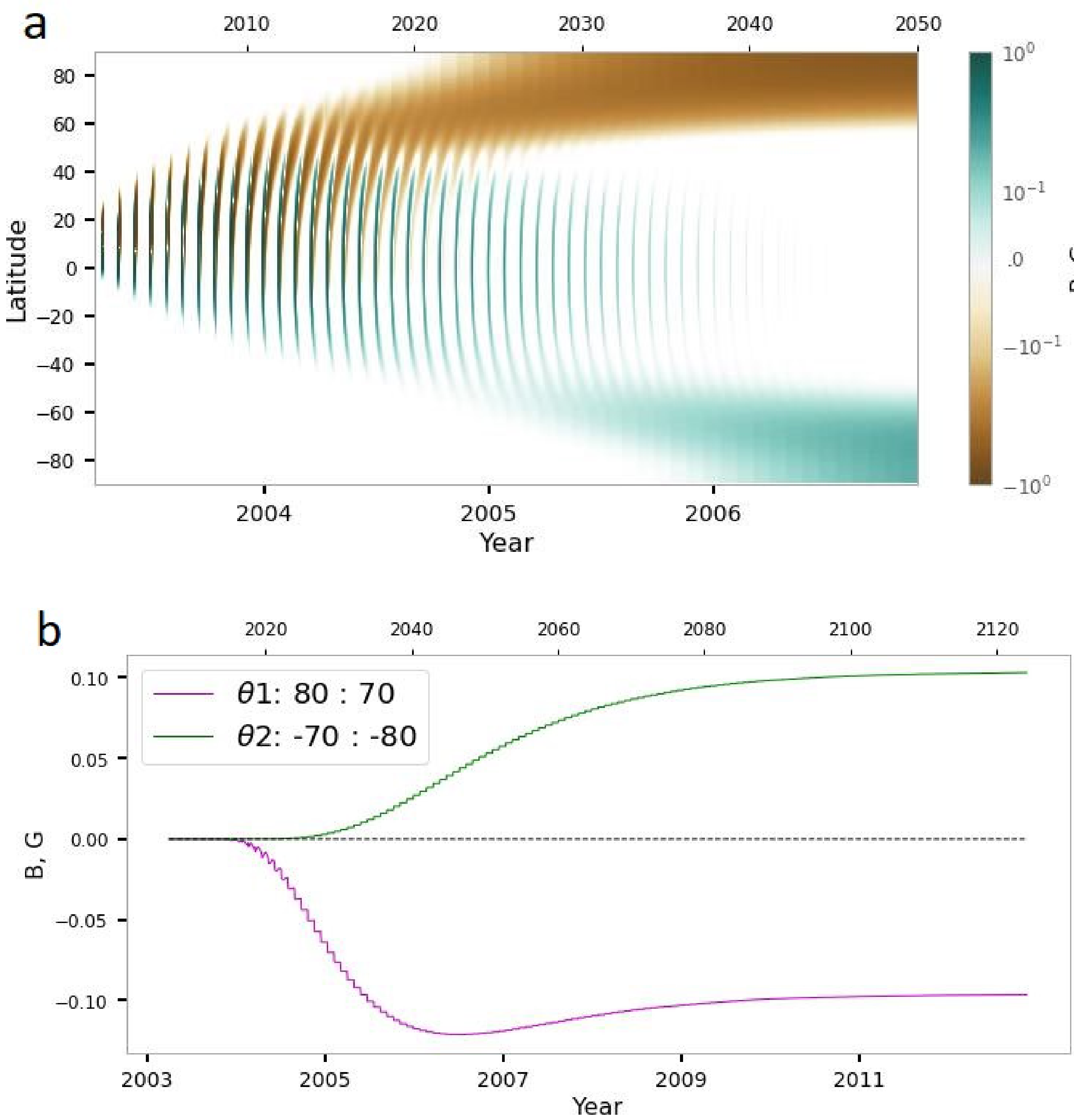
a
2010
2020
2030
2040
2050
80
60
40
20
0
−20
−40
−60
−80
Latitude
2004
2005
2006
Year
10^0
10^{-1}
.0
-10^{-1}
-10^0
B, G
b
2020
2040
2060
2080
2100
2120
0.10
0.05
0.00
−0.05
−0.10
B, G
θ1: 80 : 70
θ2: -70 : -80
2003
2005
2007
2009
2011
Year

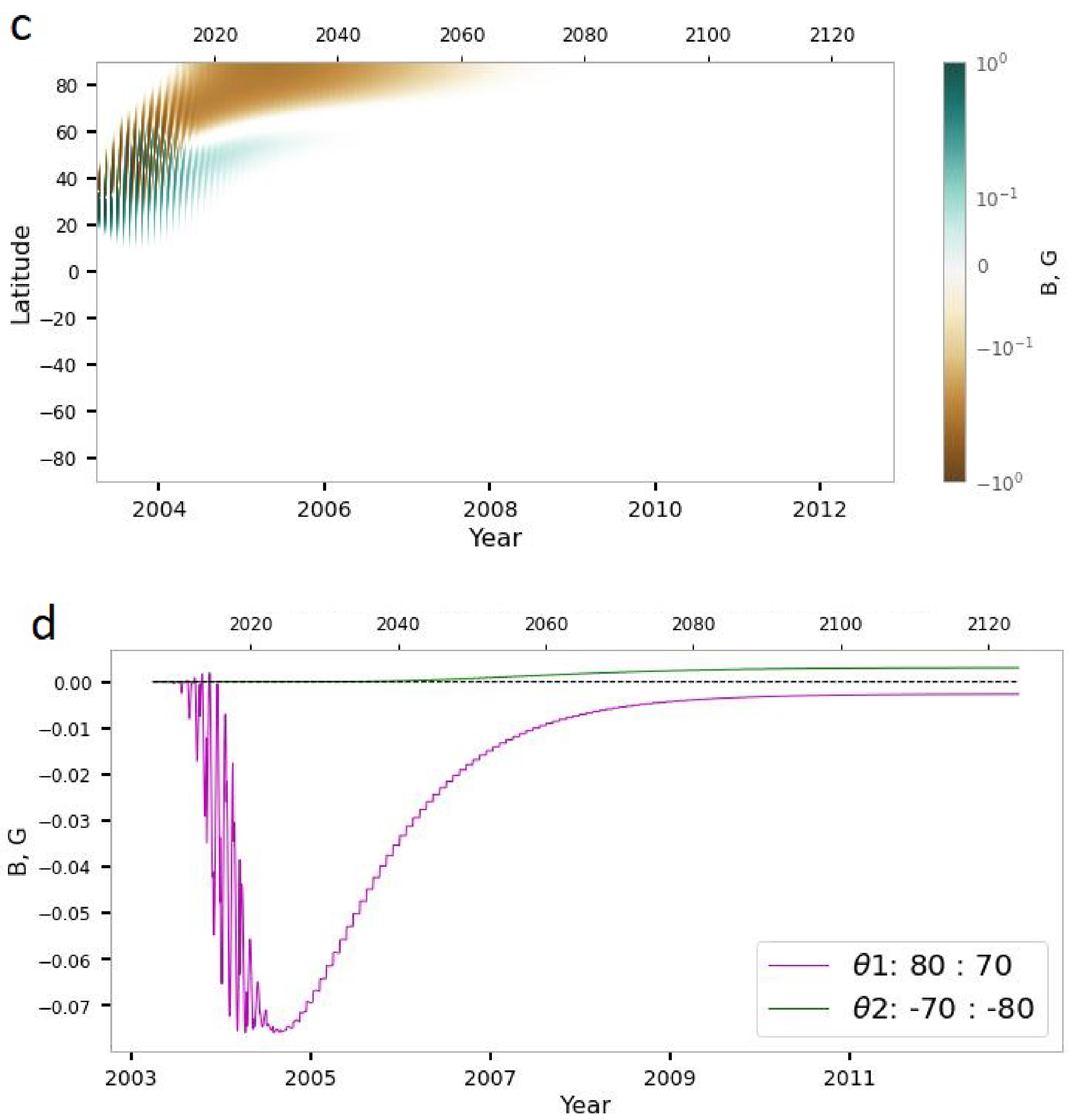
c
2020
2040
2060
2080
2100
2120
80
60
40
20
0
−20
−40
−60
−80
Latitude
2004
2006
2008
2010
2012
Year
10^0
10^{-1}
0
-10^{-1}
-10^0
B, G
d
0.00
−0.01
−0.02
−0.03
−0.04
−0.05
−0.06
−0.07
B, G
2003
2005
2007
2009
2011
Year
θ1: 80 : 70
θ2: -70 : -80

Fig. 2.

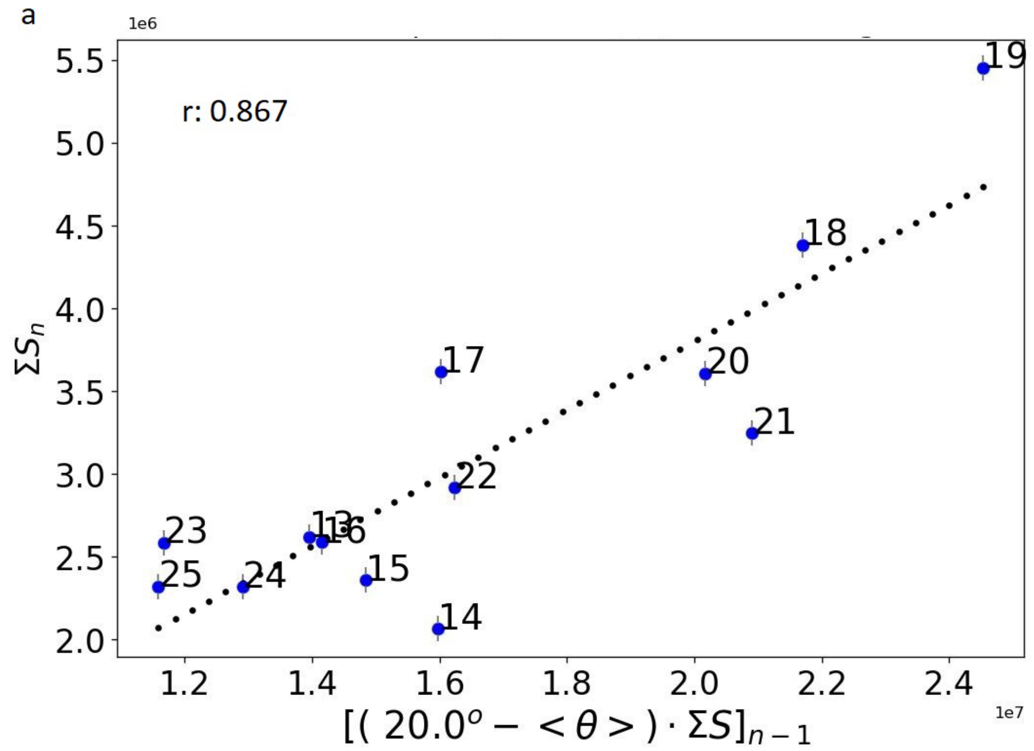
a
1e6
r: 0.867
ΣS_n
$[(\ 20.0^o - <\theta>\ ) \cdot \Sigma S]_{n-1}$
1e7
19
18
17
20
21
22
23
13
16
15
25
24
14
5.5
5.0
4.5
4.0
3.5
3.0
2.5
2.0
1.2
1.4
1.6
1.8
2.0
2.2
2.4

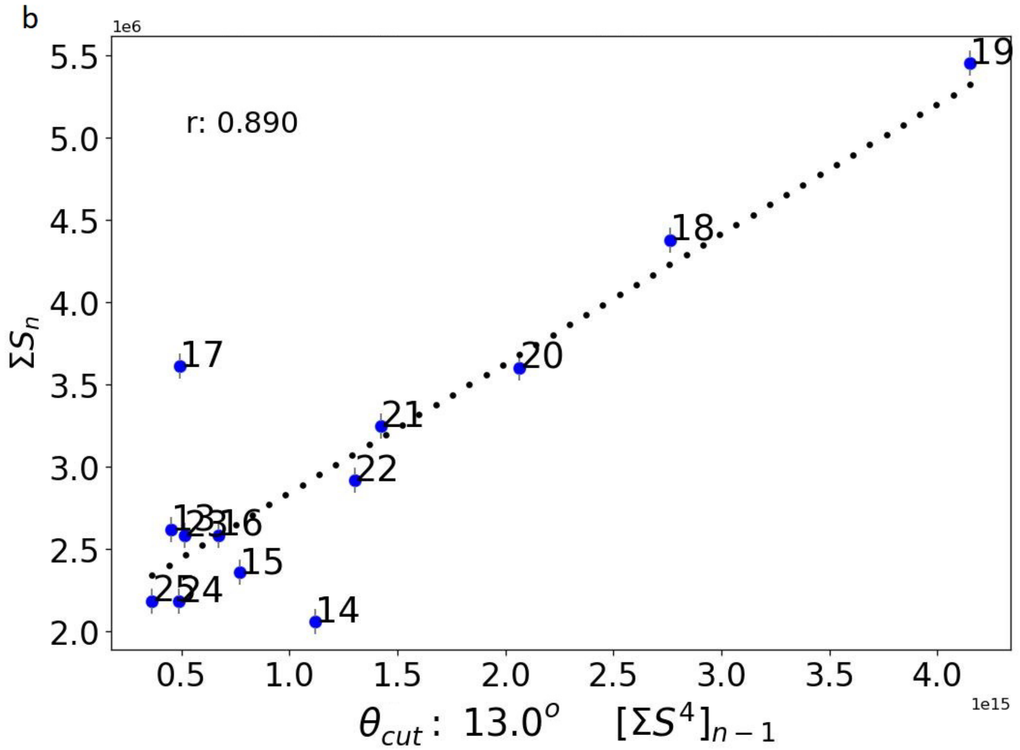
b
1e6
r: 0.890
ΣS_n
$\theta_{cut}:\ 13.0^o \quad [\Sigma S^4]_{n-1}$
1e15
19
18
17
20
21
22
16
15
24
14
5.5
5.0
4.5
4.0
3.5
3.0
2.5
2.0
0.5
1.0
1.5
2.0
2.5
3.0
3.5
4.0

Fig. 3.